Molecular Cell, Vol. 15, 703–711, September 10, 2004, Copyright ©2004 by Cell Press

Crystal Structure of the Catalytic Core of Inositol 1,4,5-Trisphosphate 3-Kinase

Gregory J. Miller and James H. Hurley*
Laboratory of Molecular Biology
National Institute of Diabetes and Digestive and Kidney Diseases
National Institutes of Health
U.S. Department of Health and Human Services
Bethesda, Maryland 20892

Summary

Soluble inositol polyphosphates are ubiquitous second messengers in eukaryotes, and their levels are regulated by an array of specialized kinases. The structure of an archetypal member of this class, inositol 1,4,5-trisphosphate 3-kinase (IP3K), has been determined at 2.2 Å resolution in complex with magnesium and adenosine diphosphate. IP3K contains a catalytic domain that is a variant of the protein kinase superfamily, and a novel four-helix substrate binding domain. The two domains are in an open conformation with respect to each other, suggesting that substrate recognition and catalysis by IP3K involves a dynamic conformational cycle. The unique helical domain of IP3K blocks access to the active site by membrane-bound phosphoinositides, explaining the structural basis for soluble inositol polyphosphate specificity.

Introduction

Inositol polyphosphates (IPs) first came to the fore as second messengers two decades ago with the discovery that inositol 1,4,5-trisphosphate (Ins(1,4,5)P_3) was the trigger for intracellular calcium mobilization (Streb et al., 1983). Recent years have seen a renaissance in soluble IP research (Abel et al., 2001; Irvine and Schell, 2001; York et al., 2001). IPs have been shown to regulate phosphoinositide-mediated protein localization (Luo et al., 2003), ion channels (Kourie et al., 1997), exocytosis of insulin granules (Efanov et al., 1997), DNA repair (Hanakahi et al., 2000), mRNA export (York et al., 1999), transcriptional regulation (Odom et al., 2000), lymphocyte development (Pouillon et al., 2003), and chromatin structure (Shen et al., 2003; Steger et al., 2003). Over 20 different soluble IPs have been shown to exist in cells. The relative levels of these IPs are controlled by IP kinases (Shears, 2004) and phosphatases (Majerus et al., 1999). Each of these enzymes is specific for either one or a small subset of related substrates. There have been steady advances in the cloning and enzymatic characterization of these enzymes in recent years, but aside from the structures of two IP phosphatases (York et al., 1994; Tsujishita et al., 2001), little is known about the structural mechanisms for their substrate specificity and site selectivity.

After Ins(1,4,5)P_3 is released from the membrane and binds to its receptor, its fate is dictated by two pathways: dephosphorylation by type I IP 5-phosphatase to inositol (1,4)P_2, or further phosphorylation by IP kinases and entry into the higher polyphosphate signaling pathways (Irvine et al., 1986). Production of inositol 1,3,4,5-tetrakisphosphate (Ins(1,3,4,5)P_4) by Ins(1,4,5)P_3 3-kinase (IP3K) is the first in a series of successive phosphorylation steps that produce inositol pentakisphosphates (IP_5), inositol hexakisphosphate (IP_6), and inositol pyrophosphates. The IP3 kinases (IP3Ks; isoforms A, B and C) have a highly conserved catalytic domain sequence, and a shared domain structure: a regulatory N terminus, a C-terminal catalytic domain, and central calmodulin binding region (Pattni and Banting, 2004; Shears, 2004). The N-terminal domains of the IP3 kinases are highly divergent, and they dictate the differential localization of these enzymes.

The catalytic domain of the IP3Ks is unrelated in primary sequence to any kinase of known structure. However, there is sequence homology to several other classes of IP kinases. These include the yeast Ins(1,4,5)P_3 6-kinase Ipk2, formerly known as Arg82 or ArgIII (Odom et al., 2000); IP_6 kinase (Saiardi et al., 1999); the multispecific rat enzyme inositol polyphosphate multikinase (Saiardi et al., 2001); and the human Ins(1,3,4,6)P_4 5-kinase (Chang et al., 2002). Because no three-dimensional structure information is available for any of these kinases, the structure of any member of the class would be invaluable as a structural template for understanding the determinants of catalysis and specificity in the larger family. Here we report the 2.2 Å structure of the conserved catalytic core of rat Ins (1,4,5)P_3 3-kinase.

Results

Overall Structure of the IP3K Catalytic Core

The structure of the IP3K catalytic core (residues 185-459 of rat IP3K-A) was determined at 2.2 Å resolution by MAD phasing from crystals of selenomethionyl protein (Figure 1A; Table 1). Residues 185-202 at the N terminus and residue 459 at the C terminus were not seen in electron density and are presumed disordered in this structure. The overall course of the main chain for residues 237-243 and residues 305-310 is discernable, but these residues are poorly ordered and were omitted from the final refined model. The construct used to obtain crystals contains two mutations, L217M and D423N. Both are conservative changes, the first in the hydrophobic core of the protein and the second on a highly solvent-exposed turn remote from the active site. The structure consists of two domains (Figure 1B). The larger domain has an α/β-class structure. The domain has an N-terminal (203-254) and a C-terminal lobe (255-264 and 327-459) with a cleft in between. Each lobe is built around an antiparallel β sheet. The sheet in the N-terminal lobe has three strands, with strand order 132. The C-terminal lobe has a five-stranded sheet with strand order 32145. The second domain (residues 265-326) is α-helical and consists of four α helices linked by long loops. The helices are loosely packed against each other and the

*Correspondence: jh8e@nih.gov

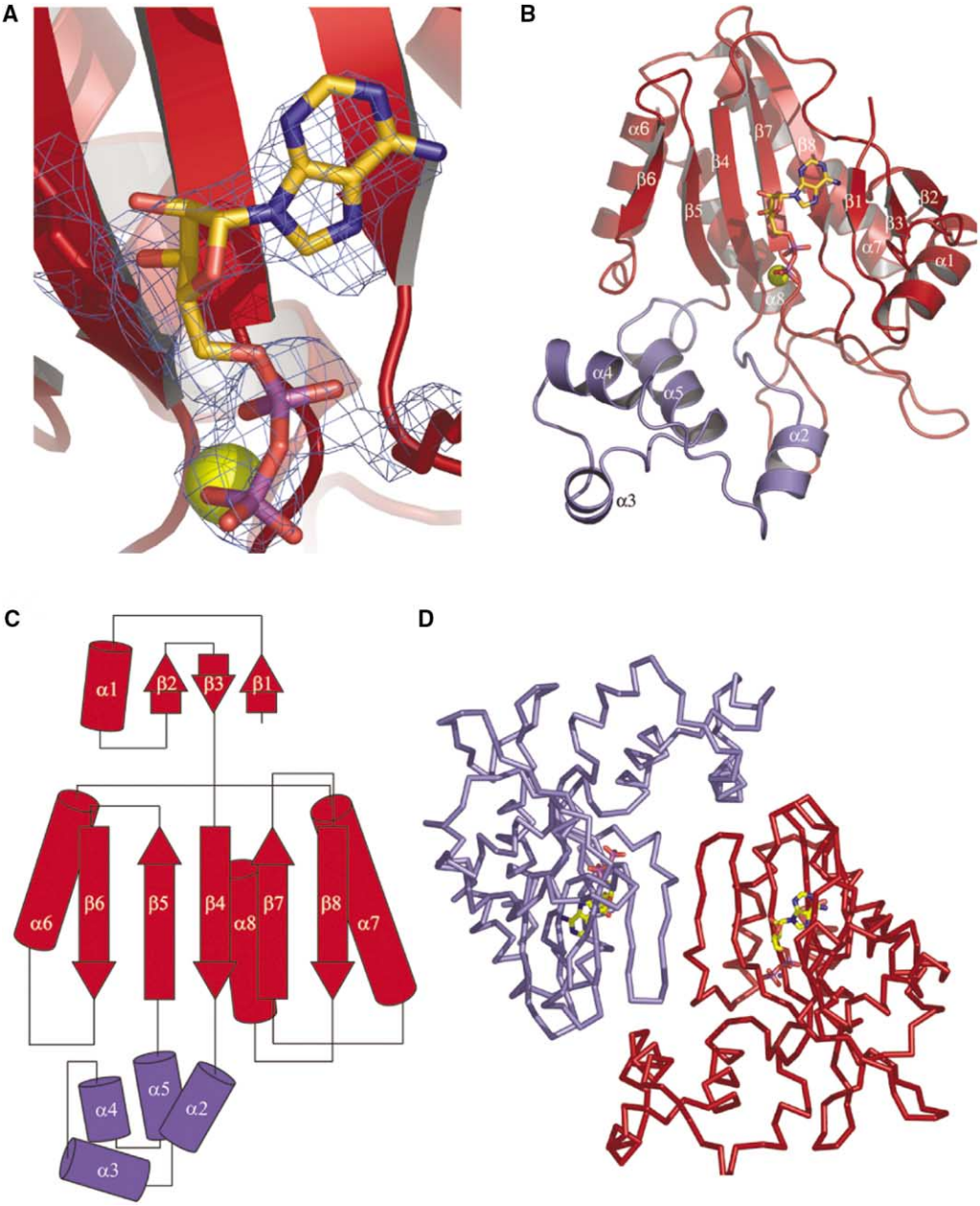

Figure 1. Structure of the Catalytic Core of Inositol 1,4,5-Trisphosphate 3-Kinase

(A) Electron density from the density modified MAD synthesis at 2.2 Å shown overlaid on the refined model of ADP. (B) Overall structure of the IP3K monomer. (C) Topology of IP3K. (D) IP3K dimer. Structural figures were prepared with Pymol (www.pymol.org).

entire domain is highly mobile as compared to the large α/β domain. The helical domain is juxtaposed against one end of the cleft in the large domain.

The catalytic core as observed in this crystal form is a dimer with non-crystallographic symmetry (Figure 1C). The β6 strands of the two monomers form an antiparallel interaction across the non-crystallographic 2-fold axis, resulting in a 10-stranded β sheet spanning the two monomers. The β5-β6 turns of each monomer contact the helical domain of their 2-fold related counterpart. The dimer buries 700 Å^2 of solvent accessible surface area per monomer. This figure is larger than usual for a crystal contact, but smaller than usual for a physiological dimer. Analytical gel filtration analysis of the IP3K core shows that the protein is a monomer in solution (not shown), at least in the absence of ligands. It will be worth exploring in the future whether dimerization is used as a mechanism for physiological inhibition.

ATP Binding Site

One molecule of ADP is bound in the cleft of the major domain, marking the active site of the kinase. The adenine base is buried in contacts with predominantly hydrophobic residues of the N-terminal lobe (Figure 2A). These include Ile-205, Pro-230, Leu-246, Leu-249, and Leu-250. Leu-399 and Ile-413 of the C-terminal lobe also

Table 1. Crystallographic Data, Phasing, and Refinement Statistics

Data Collection and Phasing		
	SeMet 1	SeMet 2
Space group	$C222_1$	$C222_1$
Unit cell (Å)	a = 72.7	a = 72.7
	b = 98.5	b = 98.5
	c = 188.7	c = 188.7
	$\alpha = \beta = \gamma = 90^\circ$	$\alpha = \beta = \gamma = 90^\circ$
Wavelength (Å)	0.9794[a]	0.9791
Resolution (Å)	50-3.0	50-2.0
Unique reflections	12702	37694
Completeness (%)	92.5	93.2
R_{merge}[b]	0.113	0.064
Anom. differences (%)	0.029-0.049	
Disp. differences (%)	0.049-0.062	
FOM (MAD)	0.39	
Refinement		
Resolution range (Å)	50.0-2.20 (2.27-2.20)	
No. of reflections	32563 (2255)[c]	
R[c] (%)	0.257 (0.251)[c]	
R_{free}[d](%)	0.305 (0.341)[c]	
Est. coordinate error (free R)	0.259	
Rms deviations:		
Bond length (Å)	0.014	
Bond angle (°)	1.8	
B factor (Å^2) main chain bonds	0.7	
B factor (Å^2) side chain bonds	2.1	
Protein atoms, number	3745	
Solvent atoms, number	632	
Ligands atoms, number	56	
Residues in allowed ϕ-Ψ region	100%	

[a] MAD data were collected at $\lambda = 0.9794$, 0.9701, 0.9118 Å. Column 1 shows representative results at $\lambda = 0.9794$. The ranges of anomalous and dispersive differences between or for the various wavelengths are provided.
[b] $R_{sym} = \Sigma_h\Sigma_i|I_i(h) - \langle I(h)\rangle|/\Sigma_h\Sigma_i I_i(h)$.
[c] Data in parentheses are for highest resolution shells.

participate in the adenine binding site. The adenine N6 is hydrogen bonded to the main-chain carbonyl of Gln-247 (Figure 2A). The ribose is held by a hydrogen bond between O3′ and Asp-260. The α-phosphate forms a charge-pair interaction with Lys-207. The α- and β-phosphates coordinate a Mg^{2+} ion together with Asp-414.

Similarity to PIPK and the Protein Kinase Superfamily

A search of known structures in the protein data bank using Dali (Holm and Sander, 1995) revealed that IP3K is a member of the protein kinase superfamily (Figures 2C, 2D, and 2E), despite the lack of significant primary sequence similarity. The highest scoring similarity is to the structure of type IIβ phosphatidylinositol phosphate kinase (PIPKIIβ; PDB file 1bo1; Rao et al., 1998). For IP3K and PIPKIIβ, a total of 131 Cα positions can be superimposed with an r.m.s.d. of 4.1 Å (Figure 3). The catalytic domain of PI 3-kinase γ (PI3Kγ, PDB file 1e8x; Walker et al., 1999), the only other lipid kinase for which a structure is available, is the tenth best hit.

Discussion

Mechanism of Inositol Polyphosphate Phosphorylation

The structure suggests a plausible mechanism for Ins(1,4,5)P_3 phosphorylation. The active site contains most of the conserved catalytic residues present in PIPKIIβ as well as counterparts of the most critical catalytic residues in protein kinase A (PKA). The bound ADP is essentially superimposable with nucleotides bound to the active site of PKA (Knighton et al., 1991a; Figure 2B). The α-phosphate binding residue Lys-72 in PKA corresponds to Lys-207. The key Glu-91 of the C-helix of PKA corresponds to Glu-213 of IP3K. The Mg^{2+} coordinating Asp184 in PKA corresponds to Asp-414 of IP3K. Lys-262 is positioned to play the same role in binding the γ-phosphate of ATP as Lys-168 of PKA, although the main-chains of the two kinases are not superimposable in this region.

In the most significant difference from both PKA and PIPK, no counterpart of the active site Asp-166 is present in the IP3Ks. Kinetic (Zhou and Adams, 1997), computational (Hutter and Helms, 1999; Valiev et al., 2003), and structural (Madhusudan et al., 2002) studies have led to the view that the Asp-166 acts as a proton trap and stabilizes the correct rotamer of the substrate Ser. Since the 3-hydroxyl of the Ins(1,4,5)P_3 is directly bonded to the sugar ring, it lacks the rotational freedom of a Ser or Thr residue. Thus the rotamer stabilization role for Asp-166 is not required in IP3K. Since all of the other critical residues of the active center are conserved, there is little doubt that the IP3K reaction proceeds by the essentially same chemical mechanism as PKA.

The structure of IP3K, the parallels with other kinases, and the model for substrate binding allow us to explain

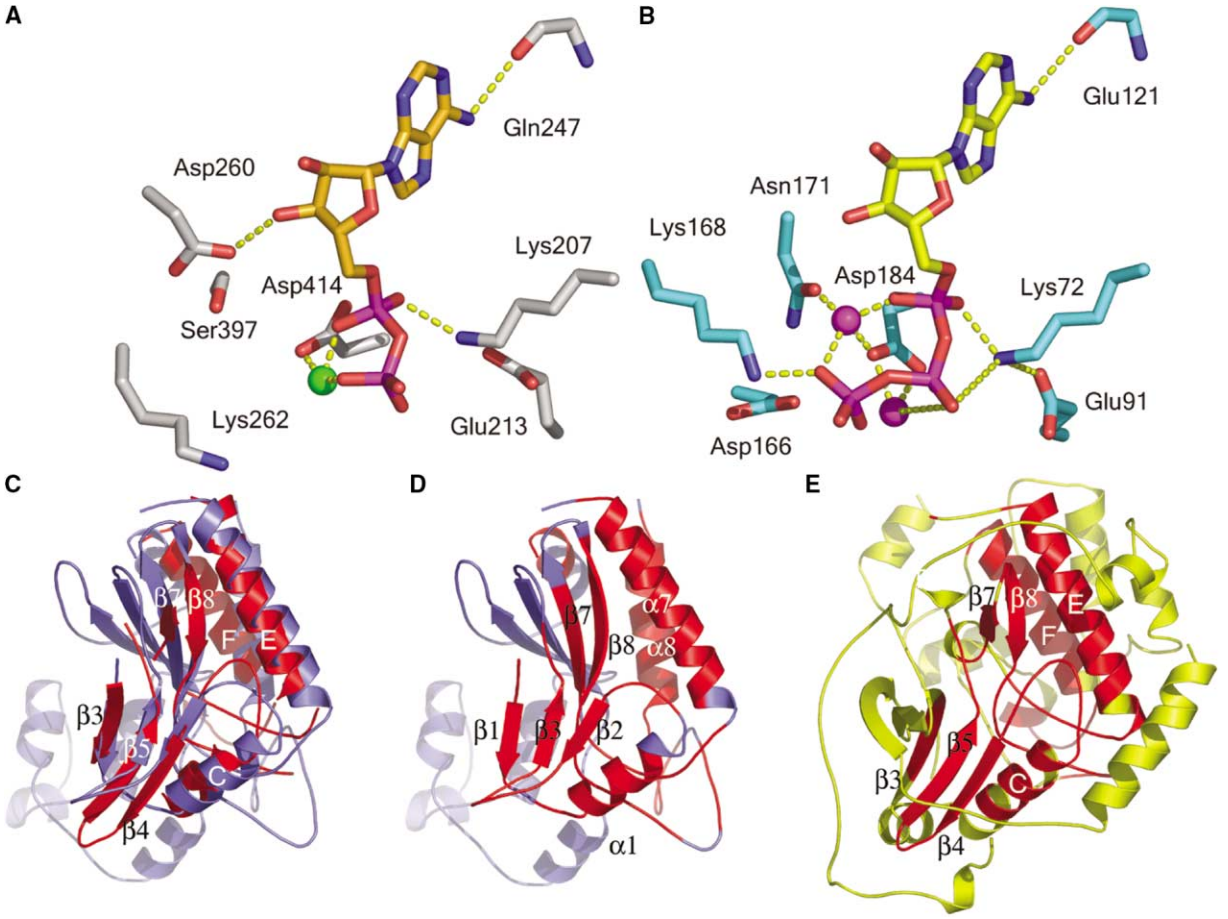

Figure 2. Structural Similarity to PKA

Side-by-side comparison of the ATP binding and catalytic sites of (A) IP3K and (B) PKA, shown in the same orientation. Atoms are colored blue (nitrogen), red (oxygen), yellow (nucleotide carbons), gray (IP3K protein carbons), cyan (PKA protein carbons), magenta (phosphorous), and green (magnesium). Hydrogen bonds and metal coordination are shown in dashed lines. (C) Overlay of IP3K (blue) with structurally homologous regions of PKA (red). (D) Structure of IP3K (blue) with regions structurally homologous to PKA colored red. (E) PKA (yellow) with regions structurally homologous to IP3K colored red.

the results of past mutational analyses (Figure 4). The IP3K mutants K197A and D414A block Mg^{2+} ATP binding (Communi et al., 1993). Asp-414 coordinates the Mg^{2+} ion that binds the α and β phosphates of ATP, and is thus essential. Lys-197 is disordered in our structure. However, the parallels with protein kinases allow us to map this Lys onto the Gly loop in the N-terminal lobe of the protein kinases. We predict that this Lys has the same function in IP3K and would become ordered upon formation of a productive substrate and ATP complex. Mutation of the ATP binding Lys-262 of IP3K (Togashi et al., 1997) and its counterpart in inositol hexakisphosphate kinase-3 (InsP6K3) abolishes catalytic activity (Saiardi et al., 2001). The motif SSLL (Ser-396 to Leu-399 in rat IP3KA) is identically conserved in IP3Ks (Figure 5) and all related IP kinases. Mutation of this motif in InsP6K3 (Saiardi et al., 2001) impair catalysis. The second Ser of the motif, Ser-397, forms a short hydrogen bond with the active site Asp-260. This Ser is conserved structurally in PIPK, although not in protein kinases, reinforcing the idea that PIPKs are the closest structural neighbors of the IP3Ks. The adjacent residues stabilize the floor of the active site. Eight mutants, seven of them of Arg or Lys residues, have been reported in the helical domain of chicken IP3K (Bertsch et al., 2000). Some increase the K_m for Ins(1,4,5)P_3, corresponding to rat IP3K-A Arg-283, Lys-310, and Arg-329. Other mutations, at the chicken counterparts of Thr-274, Arg-277, Lys-281, and Lys-284, actually decrease K_m. These K_m effects are consistent with a substrate binding role for the basic residues of the helical domain.

The crystals used in this study were grown in the presence of ADP and the reaction product Ins(1,3,4,5)P_4. While ADP is bound in the crystals, Ins(1,3,4,5)P_4 is either not bound at all, or too poorly ordered to visualize. Likewise, data collected from crystals crystallized in 10 mM Ins(1,4,5)P_3 and nucleotides fails to show evidence of Ins(1,4,5)P_3 binding. We have modeled the structure of the bound Ins(1,4,5)P_3 based on the position of the pseudosubstrate inhibitor peptide and ATP bound to PKA (Knighton et al., 1991b) (Figure 6A). One of the phosphate groups is poised to bind to Arg-317 and Lys-345. No basic ligands are unobstructed and close enough for direct interactions for the other two phosphate groups.

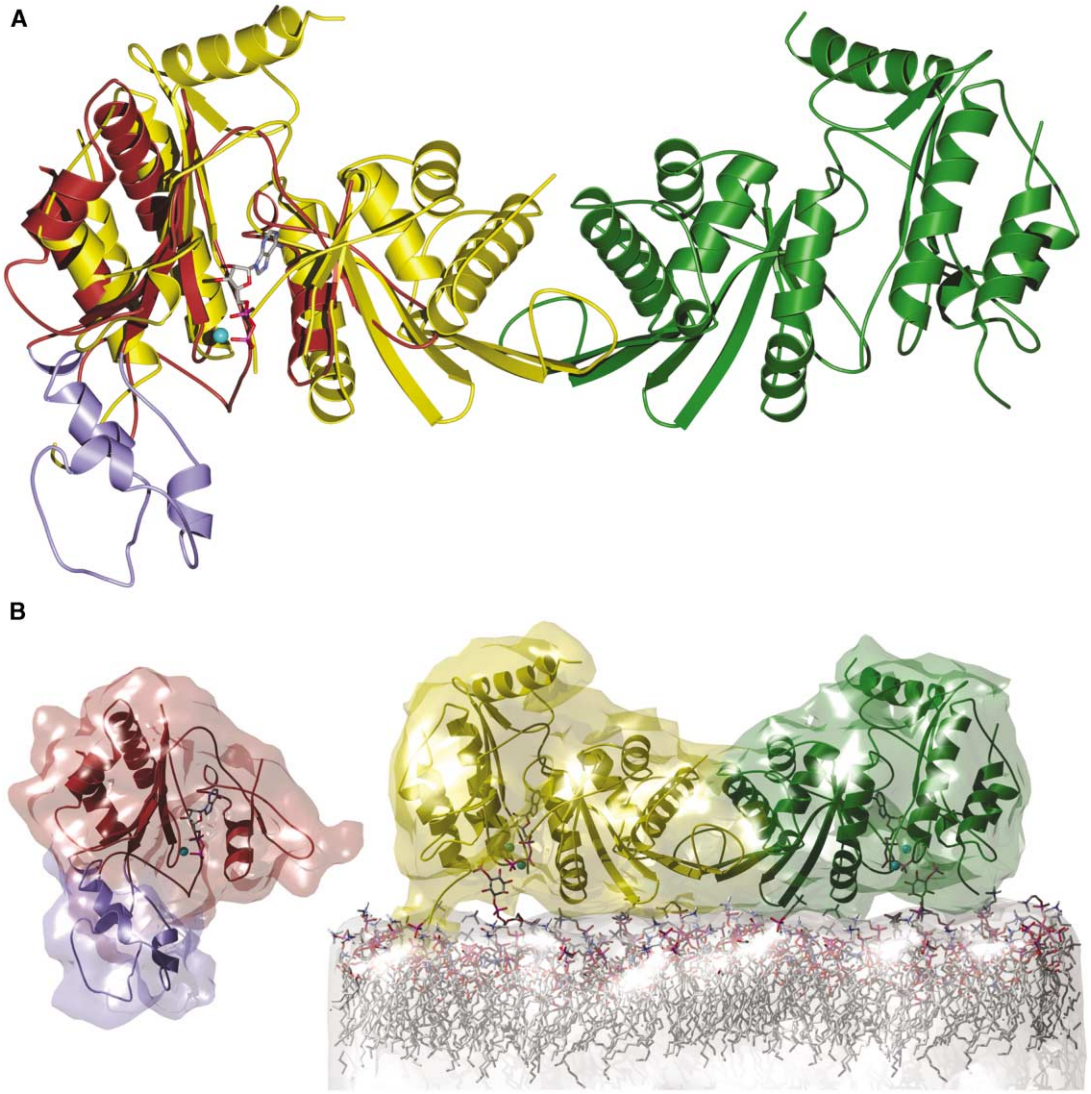

Figure 3. Structural Similarity to PIPK

(A) Three-dimensional overlay of IP3K and PIPK. Comparison of (B) IP3K and (C) PIPK shown side by side in the same orientation and with PIPK docked onto a phospholipid membrane.

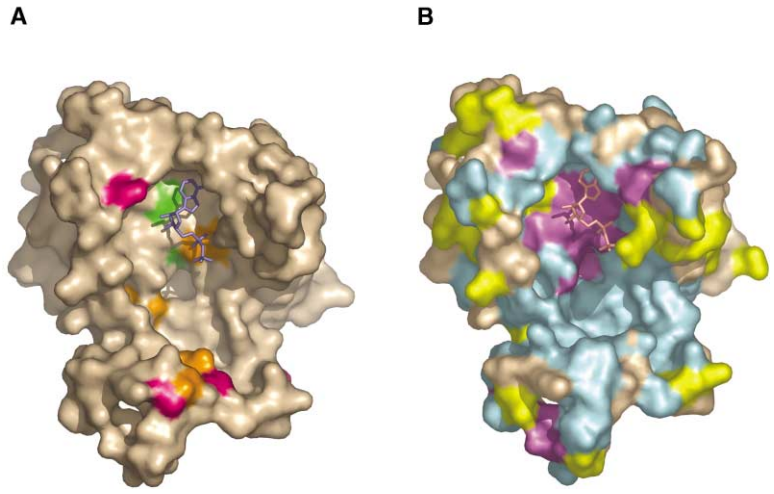

Figure 4. Conserved Residues in IP3K

(A) Mapping of mutational analysis on to the molecular surface of IP3K. Residues whose mutations enhance activity are colored pink and whose mutation impairs activity are colored orange. The SSLL motif is colored green. (B) Sequence conservation mapped onto the surface of IP3K with those residues conserved across related IP kinases colored purple, residues identical in the IP3K subfamily but not in others colored blue, and resides conserved but not identical in the IP3K subfamily colored yellow.

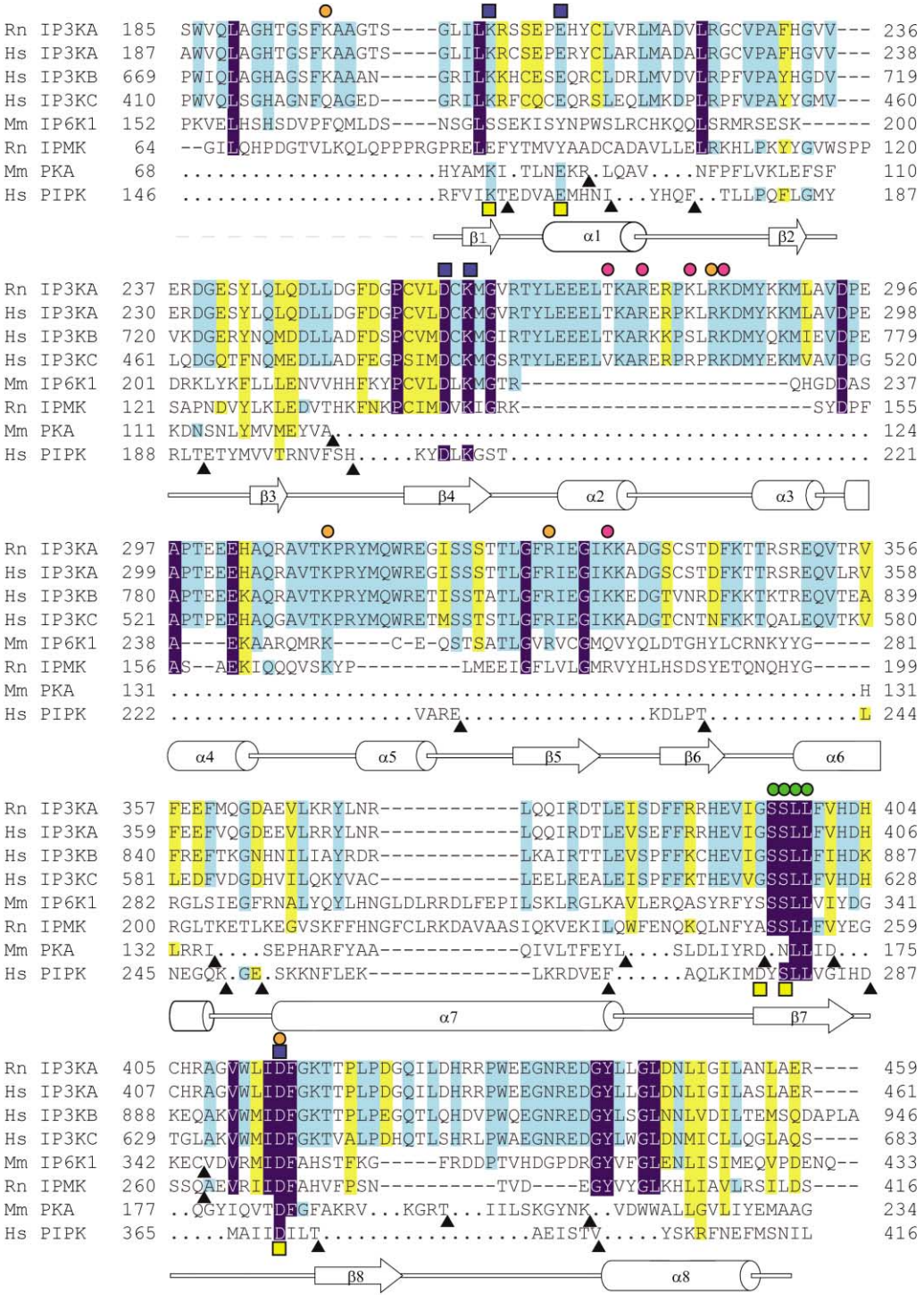

Figure 5. Structure and Sequence Alignment of IP3K and Related IP Kinases

Pink and orange dots mark residues whose mutation enhances or impairs activity, respectively. Green dots mark the SSLL motif. Shading behind conserved residues is colored as in Figure 4B. Blue and yellow squares indicate polar residues implicated in nucleotide binding and catalysis in IP3K and PKA, respectively. For PKA and PIPK, only regions that are superimposable in the three-dimensional structures are shown. Black triangles indicate positions of sequence insertions relative to IP3K.

The helical lobe is poised to bind the other two phosphates of the substrates such that they would be poised to receive the γ-phosphate group of ATP. This region of the kinase is has a net positive charge and a strongly electropositive potential (Figure 6B), as would be expected for a polyphosphate binding domain. A number of basic residues point toward the active site from the helical domain, and seven of these have been implicated

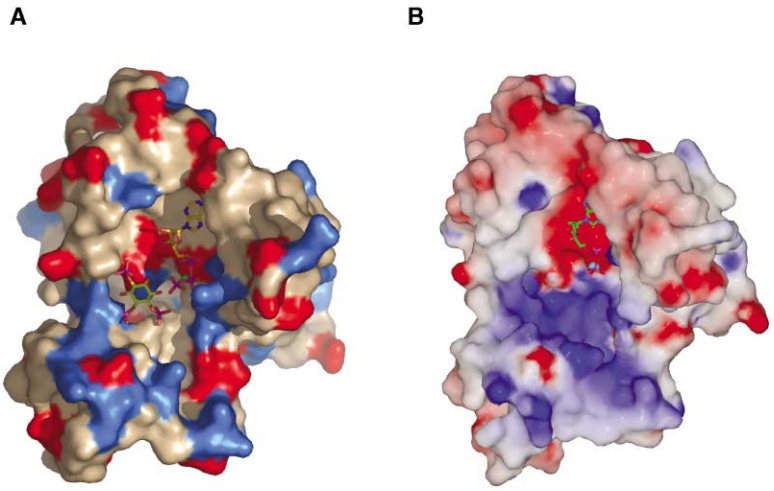

Figure 6. Modeled Substrate Binding and Surface Properties of IP3K

(A) Model of Ins (1,4,5)P_3 and ATP bound to IP3K. (B) Surface of IP3K colored by electrostatic potential, with saturating blue and red at 10 and –10 kT/e, respectively.

in substrate binding by mutagenesis. There is a gap between the modeled Ins(1,4,5)P_3 and the nearest part of the helical lobe that is too large to support direct interactions with basic residues that are known to function in substrate binding. For example, the Cα of Arg-283, which was implicated in substrate binding by mutational analysis, is 19 Å away from the active site as defined by the β-phosphate of ATP. In order to account for the mutational analysis of the helical domain and the known substrate specificity, it seems necessary that there is a domain-closing conformational change during the catalytic reaction cycle. The open conformation in this crystal form appears to have been trapped by contacts between the back side of the helical domain and the non-crystallographic symmetry-related IP3K molecule. The observed open state probably represents the trapping of one conformation among many in an ensemble of open states, and thus provides one snapshot of a dynamic conformational cycle allowing substrate binding and product release.

Soluble versus Lipid Inositide Specificity

The structural observations provide an elegant explanation for why IP3Ks phosphorylate only soluble IPs, and not membrane bound phosphoinositides. The specificity of IP3K for a soluble IP only stands in remarkable contrast to the behavior of its closest structural cousin, PIPK, which phosphorylates only membrane bound phosphoinositides. PIPK has an active site that provides relatively few direct interactions with the phosphoinositide substrate. PIPK has a very large flat basic path around the active site for docking to and binding acidic phospholipid membranes (Figure 3). The mutual affinity of PIPK and the substrate for the membrane thus drive the interaction, providing a critical enhancement to the limited interactions thought to exist between the phosphoinositide headgroup and PIPK. For this reason, PIPKs do not phosphorylate soluble IPs.

In contrast, the unique helical domain of IP3K collides with the membrane when docked in the same orientation as PIPK. Given the size of the helical domain and its insertion on what would be the membrane-proximal face of the kinase, it is not reasonable to expect that this domain could move out of the way. Thus membrane-bound phosphoinositide phosphorylation is inhibited by a direct steric blockade via the helical domain. The enzyme inositol polyphosphate multikinase (IPMK) is homologous to IP3K and has membrane PI 3-kinase activity (S. Snyder, personal communication). In the IPMK sequence, essentially all of the helical lobe is absent (Figure 5). Thus IPMK would be expected on structural grounds to have free access to membrane-bound substrates. The parallels between these lipid phosphoinositide, soluble IP, and mixed specificity kinases highlight the IP3K/PIPK fold as a versatile scaffold for the phosphorylation of diverse soluble and lipophilic inositol compounds.

Experimental Procedures

DNA Constructs

A DNA fragment encoding residues 185-459 of the rat inositol 1,4,5-trisphosphate 3-kinase type A catalytic domain (Choi et al., 1990; Takazawa et al., 1990) was generated by PCR amplification and successively cloned into the pDONOR201 vector and then the pDEST-15 vector (Invitrogen). The construct used for crystallization was sequenced and contains the mutations L217M and D423N.

Protein Expression, Purification, and Crystallization

The native and SeMet IP3KA-185-459 domains were expressed as GST-tagged fusion proteins, the native protein in *Escherichia coli* strain Rosetta (DE3) (Novagen) and the SeMet derivative in BL834 (Novagen). Both were purified by affinity chromatography using glutathione-Sepharose (Amersham Pharmacia). The column was washed with 10 column volumes of 10 mM Na phosphate (pH 7.4) and 150 mM NaCl followed by 10 column volumes of 10 mM Na phosphate (pH 7.4) and 500 mM NaCl. The fusion protein was eluted in 10 mM phosphate buffer and 150 mM NaCl with 20 mM glutathione. During dialysis, the GST tags were removed with recombinant TEV protease and the proteins were subjected to a second purification using glutathione-Sepharose. Following concentration, ammonium sulfate was added to a final concentration of 1.25 M and the proteins were purified on a PHE15 SOURCE column (Amersham-Pharmacia) and eluted over a gradient of decreasing ammonium sulfate concentration. The proteins were further purified using a Superdex 200 26/60 gel filtration column (Amersham-Pharmacia) equilibrated with 25 mM Tris-HCl (pH 8.0), 150 mM NaCl, and 10 mM DTT. Both native and SeMet proteins were concentrated to 10 mg ml^{-1} for use in crystallization trials.

The SeMet protein crystallized in 2.2 M ammonium sulfate, 0.2 M Na formate, 10 mM DTT, 10 mM ADP, 10 mM Ins (1,3,4,5)P4, and

10 mM $MgCl_2$. The crystals were cryoprotected by the successive transfer of the crystals into mother liquor containing 5%, 10%, and 15% glycerol.

X-Ray Data Collection and Structure Determination

A three-wavelength multiwavelength anomalous dispersion (MAD) data set (Table 1, SeMet 1) was collected from crystals frozen in liquid nitrogen at beamline 9-2, Stanford Synchrotron Radiation Laboratory (Menlo Park, CA). Data were collected in 0.5 degree oscillations for 5–10 s per exposure on an ADSC 315 CCD detector and processed with HKL2000 (Otwinowski and Minor, 1997). Twelve Se positions were located with SOLVE (Terwilliger and Berendzen, 1999) and a 3.0 Å MAD map was calculated. A single wavelength data set was collected from a second SeMet IP3K crystal at 2.0 Å resolution (Table 1, SeMet 2). The initial map was improved by solvent flattening, 2-fold non-crystallographic symmetry averaging and phase extension to 2.2 Å in RESOLVE (Terwilliger, 2000). The resulting 2.2 Å map was interpreted with O (Jones et al., 1991). Refinement was carried out initially using torsional dynamics in CNS (Brunger et al., 1998), and then using TLS refinement (Winn et al., 2001) in Refmac5 (Murshudov et al., 1997). For TLS refinement, the N and C-terminal lobes of the kinase domain of each monomer in the asymmetric unit were treated as single units, and the helical domains were each broken into three units.

Acknowledgments

We thank Richard A. Anderson for providing DNAs and for first suggesting this line of research to us; Solomon Snyder for communicating prepublication information; Susan Taylor for helpful discussions; Darrell Hurt and Gali Prag for assistance with figure preparation; Bertram Canagarajah for computational support; and Jaewon Kim, Gali Prag, Aitor Hierro, Don Ronning, and the staff of beamline 9-2, Stanford Synchrotron Radiation Laboratory (Menlo Park, CA) for assistance with x-ray data collection and for access to beam time.

Received: June 16, 2004
Revised: July 12, 2004
Accepted: July 14, 2004
Published online: August 12, 2004

References

Abel, K., Anderson, R.A., and Shears, S.B. (2001). Phosphatidylinositol and inositol phosphate metabolism. J. Cell Sci. *114*, 2207–2208.

Bertsch, U., Deschermeier, C., Fanick, W., Girkontaite, I., Hillemeier, K., Johnen, H., Weglohner, W., Emmrich, F., and Mayr, G.W. (2000). The second messenger binding site of inositol 1,4,5-trisphosphate 3-kinase is centered in the catalytic domain and related to the inositol trisphosphate receptor site. J. Biol. Chem. *275*, 1557–1564.

Brunger, A.T., Adams, P.D., Clore, G.M., DeLano, W.L., Gros, P., Grosse-Kunstleve, R.W., Jiang, J.S., Kuszewski, J., Nilges, M., Pannu, N.S., et al. (1998). Crystallography & NMR system: a new software suite for macromolecular structure determination. Acta Crystallogr. D *54*, 905–921.

Chang, S.C., Miller, A.L., Feng, Y., Wente, S.R., and Majerus, P.W. (2002). The human homolog of the rat inositol phosphate multikinase is an inositol 1,3,4,6-tetrakisphosphate 5-kinase. J. Biol. Chem. *277*, 43836–43843.

Choi, K.Y., Kim, H.K., Lee, S.Y., Moon, K.H., Sim, S.S., Kim, J.W., Chung, H.K., and Rhee, S.G. (1990). Molecular-cloning and expression of a complementary-DNA for inositol 1,4,5-trisphosphate 3-kinase. Science *248*, 64–66.

Communi, D., Takazawa, K., and Erneux, C. (1993). Lys-197 and Asp-414 are critical residues for binding of ATP/Mg2+ by rat brain inositol 1,4,5-trisphosphate 3-kinase. Biochem. J. *291*, 811–816.

Efanov, A.M., Zaitsev, S.V., and Berggren, P.O. (1997). Inositol hexakisphosphate stimulates non-Ca2+-mediated and primes Ca2+-mediated exocytosis of insulin by activation of protein kinase C. Proc. Natl. Acad. Sci. USA *94*, 4435–4439.

Hanakahi, L.A., Bartlet-Jones, M., Chappell, C., Pappin, D., and West, S.C. (2000). Binding of inositol phosphate to DNA-PK and stimulation of double-strand break repair. Cell *102*, 721–729.

Holm, L., and Sander, C. (1995). Dali-a network tool for protein-structure comparison. Trends Biochem. Sci. *20*, 478–480.

Hutter, M.C., and Helms, V. (1999). Influence of key residues on the reaction mechanism of the cAMP-dependent protein kinase. Protein Sci. *8*, 2728–2733.

Irvine, R.F., and Schell, M.J. (2001). Back in the water: The return of the inositol phosphates. Nat. Rev. Mol. Cell Biol. *2*, 327–338.

Irvine, R.F., Letcher, A.J., Heslop, J.P., and Berridge, M.J. (1986). The inositol tris/tetrakisphosphate pathway-demonstration of Ins(1,4,5)P3 3-kinase activity in animal tissues. Nature *320*, 631–634.

Jones, T.A., Zou, J.Y., Cowan, S.W., and Kjeldgaard, M. (1991). Improved methods for building protein models in electron-density maps and the location of errors in these models. Acta Crystallogr. A *47*, 110–119.

Knighton, D.R., Zheng, J.H., Teneyck, L.F., Ashford, V.A., Xuong, N.H., Taylor, S.S., and Sowadski, J.M. (1991a). Crystal-structure of the catalytic subunit of cyclic adenosine-monophosphate dependent protein-kinase. Science *253*, 407–414.

Knighton, D.R., Zheng, J.H., Teneyck, L.F., Xuong, N.H., Taylor, S.S., and Sowadski, J.M. (1991b). Structure of a Peptide Inhibitor Bound to the Catalytic Subunit of Cyclic Adenosine-Monophosphate Dependent Protein-Kinase. Science *253*, 414–420.

Kourie, J.I., Foster, P.S., and Dulhunty, A.F. (1997). Inositol polyphosphates modify the kinetics of a small chloride channel in skeletal muscle sarcoplasmic reticulum. J. Membr. Biol. *157*, 147–158.

Luo, H.R., Huang, Y.E., Chen, J.C., Saiardi, A., Iijima, M., Ye, K., Huang, Y., Nagata, E., Devreotes, P., and Snyder, S.H. (2003). Inositol pyrophosphates mediate chemotaxis in Dictyostelium via pleckstrin homology domain-PtdIns(3,4,5)P3 interactions. Cell *114*, 559–572.

Madhusudan, Akamine, P., Xuong, N.H., and Taylor, S.S. (2002). Crystal structure of a transition state mimic of the catalytic subunit of cAMP-dependent protein kinase. Nat. Struct. Biol. *9*, 273–277.

Majerus, P.W., Kisseleva, M.V., and Norris, F.A. (1999). The role of phosphatases in inositol signaling reactions. J. Biol. Chem. *274*, 10669–10672.

Murshudov, G.N., Vagin, A.A., and Dodson, E.J. (1997). Refinement of macromolecular structures by the maximum-likelihood method. Acta Crystallogr. D *53*, 240–255.

Odom, A.R., Stahlberg, A., Wente, S.R., and York, J.D. (2000). A role for nuclear inositol 1,4,5-trisphosphate kinase in transcriptional control. Science *287*, 2026–2029.

Otwinowski, Z., and Minor, W. (1997). Processing of X-ray diffraction data collected in oscillation mode. In Macromolecular Crystallography, Pt A, pp. 307–326.

Pattni, K., and Banting, G. (2004). Ins(1,4,5)P3 metabolism and the family of IP3-3Kinases. Cell. Signal. *16*, 643–654.

Pouillon, V., Hascakova-Bartova, R., Pajak, B., Adam, E., Bex, F., Dewaste, V., Van Lint, C., Leo, O., Erneux, C., and Schurmans, S. (2003). Inositol 1,3,4,5-tetrakisphosphate is essential for T lymphocyte development. Nat. Immunol. *4*, 1136–1143.

Rao, V.D., Misra, S., Boronenkov, I.V., Anderson, R.A., and Hurley, J.H. (1998). Structure of type II beta phosphatidylinositol phosphate kinase: a protein kinase fold flattened for interfacial phosphorylation. Cell *94*, 829–839.

Saiardi, A., Erdjument-Bromage, H., Snowman, A.M., Tempst, P., and Snyder, S.H. (1999). Synthesis of diphosphoinositol pentakisphosphate by a newly identified family of higher inositol polyphosphate kinases. Curr. Biol. *9*, 1323–1326.

Saiardi, A., Nagata, E., Luo, H.R., Sawa, A., Luo, X., Snowman, A.M., and Snyder, S.H. (2001). Mammalian inositol polyphosphate multikinase synthesizes inositol 1,4,5-trisphosphate and an inositol pyrophosphate. Proc. Natl. Acad. Sci. USA *98*, 2306–2311.

Shears, S.B. (2004). How versatile are inositol phosphate kinases? Biochem. J. *377*, 265–280.

Shen, X., Xiao, H., Ranallo, R., Wu, W.H., and Wu, C. (2003). Modulation of ATP-dependent chromatin-remodeling complexes by inositol polyphosphates. Science *299*, 112–114.

Steger, D.J., Haswell, E.S., Miller, A.L., Wente, S.R., and O'Shea, E.K. (2003). Regulation of chromatin remodeling by inositol polyphosphates. Science *299*, 114–116.

Streb, H., Irvine, R.F., Berridge, M.J., and Schulz, I. (1983). Release of Ca2+ from a nonmitochondrial intracellular store in pancreatic acinar cells by inositol-1,4,5-trisphosphate. Nature *306*, 67–69.

Takazawa, K., Vandekerckhove, J., Dumont, J.E., and Erneux, C. (1990). Cloning and expression in escherichia coli of a rat-brain Cdna-encoding a Ca-2+/calmodulin-sensitive inositol 1,4,5-trisphosphate 3-kinase. Biochem. J. *272*, 107–112.

Terwilliger, T.C. (2000). Maximum-likelihood density modification. Acta Crystallogr. D *56*, 965–972.

Terwilliger, T.C., and Berendzen, J. (1999). Automated MAD and MIR structure solution. Acta Crystallogr. D *55*, 849–861.

Togashi, S., Takazawa, K., Endo, T., Erneux, C., and Onaya, T. (1997). Structural identification of the myo-inositol 1,4,5-trisphosphate-binding domain in rat brain inositol 1,4,5-trisphosphate 8-kinase. Biochem. J. *326*, 221–225.

Tsujishita, Y., Guo, S.L., Stolz, L.E., York, J.D., and Hurley, J.H. (2001). Specificity determinants in phosphoinositide dephosphorylation: crystal structure of an archetypal inositol polyphosphate 5-phosphatase. Cell *105*, 379–389.

Valiev, M., Kawai, R., Adams, J.A., and Weare, J.H. (2003). The role of the putative catalytic base in the phosphoryl transfer reaction in a protein kinase: First-principles calculations. J. Am. Chem. Soc. *125*, 9926–9927.

Walker, E.H., Perisic, O., Ried, C., Stephens, L., and Williams, R.L. (1999). Structural insights into phosphoinositide 3-kinase catalysis and signalling. Nature *402*, 313–320.

Winn, M.D., Isupov, M.N., and Murshudov, G.N. (2001). Use of TLS parameters to model anisotropic displacements in macromolecular refinement. Acta Crystallogr. D *57*, 122–133.

York, J.D., Ponder, J.W., Chen, Z.W., Mathews, F.S., and Majerus, P.W. (1994). Crystal-Structure of Inositol Polyphosphate 1-Phosphatase at 2.3-Angstrom Resolution. Biochemistry *33*, 13164–13171.

York, J.D., Odom, A.R., Murphy, R., Ives, E.B., and Wente, S.R. (1999). A phospholipase C-dependent inositol polyphosphate kinase pathway required for efficient messenger RNA export. Science *285*, 96–100.

York, J.D., Guo, S.L., Odom, A.R., Spiegelberg, B.D., and Stolz, L.E. (2001). An expanded view of inositol signaling. In Advances in Enzyme Regulation. Vol *41*, 57–71.

Zhou, J., and Adams, J.A. (1997). Is there a catalytic base in the active site of cAMP-dependent protein kinase? Biochemistry *36*, 2977–2984.

Accession Numbers

Coordinates have been deposited in the Protein Data Bank with the accession code 1TZD.